

Luminescence Properties of Si-Containing Porous Matrix–PbS Nanoparticle Systems

S. A. Tarasov^a, O.A. Aleksandrova^a, I. A. Lamkin^a, A. I. Maksimov^a, E. V. Maraeva^a, I. I. Mikhailov^a, V. A. Moshnikov^{a,b}, S. F. Musikhin^b, S. S. Nalimova^a, N. V. Permyakov^a, Yu. M. Spivak^a, and P. G. Travkin^a

^aSt. Petersburg State Electrotechnical University “LETI”, St. Petersburg, 197376 Russia

^bSt. Petersburg State Polytechnic University, St. Petersburg, 195251 Russia

e-mail: satarasov@mail.ru

Submitted April 10, 2014

Abstract—The luminescence properties of systems that contain lead-sulfide nanoparticles deposited onto substrates fabricated from porous silicon, oxidized porous silicon, and porous (tin-oxide)–(silicon-oxide) layers are studied. It is shown that the structure and composition of the matrix induce a strong effect on the luminescence spectra of colloidal quantum dots, defining their emission wavelength.

Keywords: colloidal quantum dots, photoluminescence, porous silicon-containing matrices, lead chalcogenides.

DOI: 10.1134/S1063782615130138

At present, much attention is given to hybrid quantum dot–porous matrix systems. Such composite materials are used in medicine and offer promise for the production of solar cells and photodetectors. The advantages of quantum dots in porous matrices are their size stability and high densities of emitting centers.

In this study, we explore hybrid systems produced by the deposition of a solution of lead-sulfide colloidal (PbS) quantum dots (QDs) [1–4] onto porous-silicon- (por-Si) [5–7] and silicon-dioxide substrates [8–10]. We used three types of Si-based substrates: single-crystal Si (type 1), por-Si (type 2), and por-Si subjected to oxidation in air for 14 days (type 3). Porous silicon was produced by anodic electrochemical etching in a one-chamber cell, in an electrolyte based on an aqueous solution of hydrogen fluoride with the addition of isopropyl alcohol. As substrates, we used (111)-oriented *n*-Si:P wafers with a resistivity of 5 Ω cm. Figure 1 shows a typical image of the resultant por-Si surface. The pore diameter was varied in the range 10–40 nm.

The luminescence spectra were studied using an installation created on the basis of an SDL-1 high-resolution double-grating diffraction monochromator. For the excitation-radiation source, we used a Nd:YVO₄ solid-state laser with diode pumping and frequency doubling ($\lambda = 532$ nm) and a semiconductor laser diode emitting at the wavelength $\lambda = 445$ nm.

The PbS colloidal QDs (CQDs) to be studied were synthesized by the pyrolysis of metal-organic compounds (lead oleate and others) with organic systems in contact with a source of sulfur. Figure 2 shows the typical absorption and luminescence spectra of the CQDs. A small shift of the emission peak with respect to the first exciton peak in the absorption spectrum (a small Stokes shift) is indicative of a low degree of particle imperfection. We studied two types of samples (PbS 935 and PbS 950) different in QD size (Fig. 3a), as demonstrated by the difference between the peak positions in the emission spectra. In this case, for par-

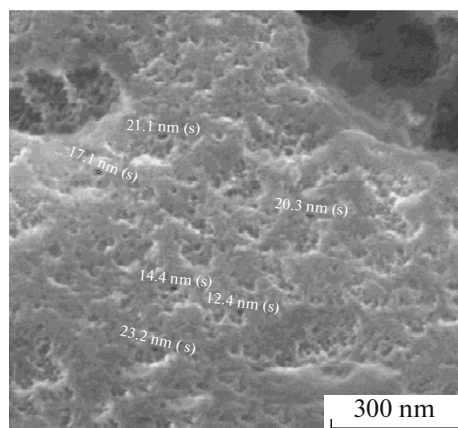


Fig. 1. Image of the surface of por-Si (250000× magnification).

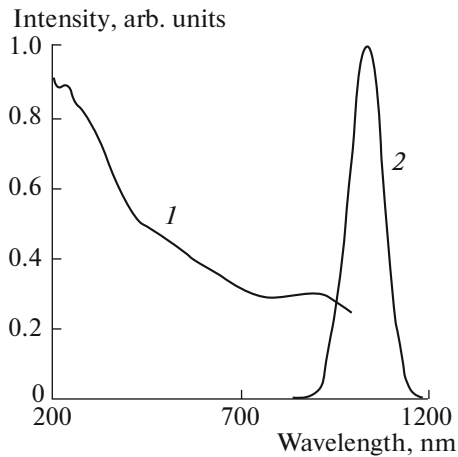


Fig. 2. Absorption (curve 1) and luminescence (curve 2) spectra of PbS CQDs (type 935).

ticles embedded in liquid media, the difference between the peak positions in the emission spectra exceeded 35 nm.

The deposition of PbS nanoparticles onto porous Si-containing matrices influences the luminescence spectrum in different ways. The deposition of QDs onto por-Si substrates immediately after anodization does not yield any substantial changes in the luminescence spectrum of the QDs (Fig. 4a). If we use por-Si substrates oxidized in air, we observe a shift of the luminescence peak to shorter wavelengths.

The shift of the luminescence spectrum can be explained in the manner described below. The initial colloidal solution contains QDs of different sizes. The pore sizes in the unoxidized substrate can be too large to induce a significant influence on the dimensions of nanoparticles entering the pores. In the case of the oxidized por-Si substrate, the pore dimensions are decreased because of oxide formation. As a result, only

small nanoparticles enter the pores; i.e., particles are selected by their size. In addition, during the deposition and distribution of nanoparticles over the substrate surface, the nanoparticles experience capillary or other forces. Therefore, coarser particles can break down, which is accompanied by the selection of smaller particles. This results in a shift of the luminescence peak to shorter wavelengths. In this case, the initial particle size barely influences the size of QDs deposited onto the oxidized porous matrix. This inference follows from the fact that the emission spectra of deposited particles of different types are almost identical (Fig. 3b).

The deposition of PbS CQDs onto a por-Si surface modifies the photoluminescence (PL) spectra of the substrate material itself. Figure 4b shows the PL spectrum of por-Si samples without nanoparticles and the spectra of oxidized por-Si structures with PbSe CQDs deposited onto the surface. The luminescence of por-Si is associated with emission from Si nanorods and nanowalls [6] and partially with emission involving surface states. Upon the addition of QDs, the QDs fill pores and become located at the surface of such rods and walls, which modifies the wave functions of Si nanostructures and the positions of energy levels, thus inducing the splitting or broadening of levels. In this case, the effective band gap decreases, and the luminescence peak shifts to longer wavelengths. This effect is similar to the effect of the interaction of two coupled quantum wells (QWs). In this case, the levels split, and the lower level appears to be lower than the position of the level in a single QW. The position of levels depends on the thickness of the barrier between the QWs. If the barrier is very thin, the system transforms into a QW, whose width is twice that of the initial QW, and the levels of the new QW are lower. Estimation of the width of such a QW and the position of levels shows satisfactory agreement of the results with the experimental results. The estimate was obtained starting

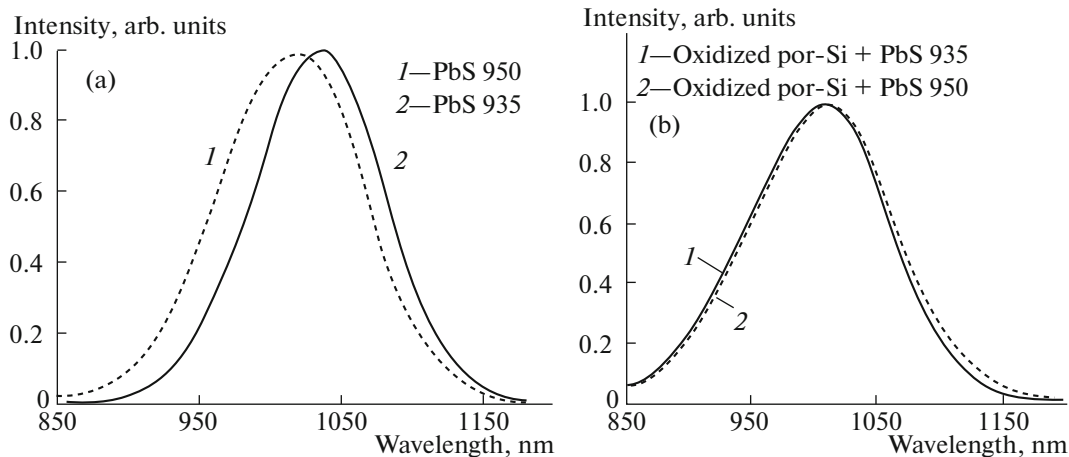


Fig. 3. PL spectra of PbS CQDs (a) located in solutions and (b) deposited onto substrates.

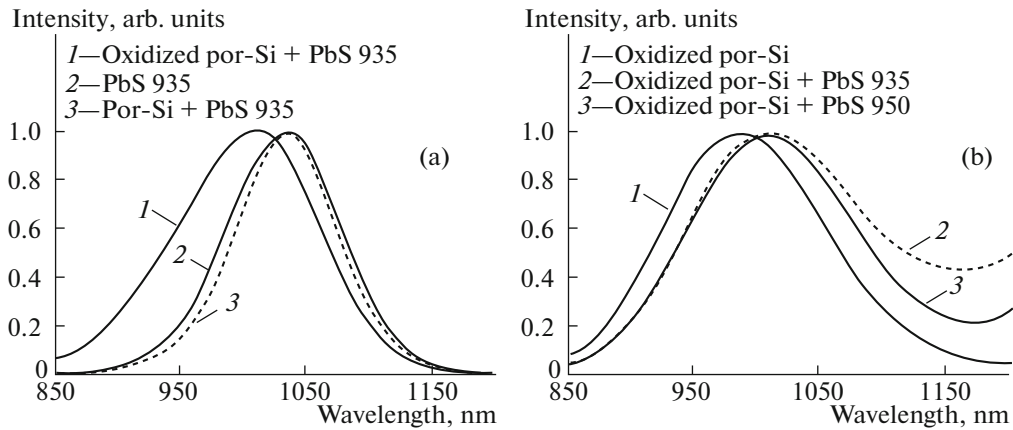


Fig. 4. Luminescence spectra of (a) PbS CQDs deposited onto porous substrates or located in solutions and (b) oxidized substrates with and without deposited QDs.

from the energy position of the PL peak and the electron and hole effective masses and using the expression

$$h\nu = E_g + \frac{\pi^2 \hbar^2}{2m_1 d^2} + \frac{\pi^2 \hbar^2}{2m_2 d^2}.$$

Here, $h\nu$ is the energy corresponding to the luminescence peak; E_g is the band gap of “classical” silicon; m_1 and m_2 are, correspondingly, the electron and hole effective masses; and d is the QW width.

The estimated QW width is 1.2 nm. In the case of samples with deposited QDs, the effective masses of charge carriers in PbS are substituted into the above expression. For such samples, the QW width is 3.190 nm.

Along with por-Si, the basic system $\text{SiO}_2\text{--SnO}_2$ was considered [8]. We used a four-layer 90%

$\text{SnO}_2\text{--}10\% \text{SiO}_2$ matrix fabricated on a glassy quartz substrate by the sol–gel technique. The layers were deposited by centrifugation at a rate of 3000 rpm over 15 s. After the deposition of each layer, we conducted annealing at a temperature 600°C for 5 min. The final four-layer structure was annealed at the same temperature for 30 min. Figure 5 shows the atomic-force microscopy (AFM) image of a single-layer sample produced under the same conditions. As in por-Si, there are relatively large pores (about 200 nm in dimensions) as well as small pores in the isthmuses between large pores.

In addition, we fabricated a sample, in which only the final structure was annealed, whereas individual layers when deposited were dried in air. Such a structure is bound to present a nonporous tin-dioxide phase similar to a glass. As in por-Si, in this case, we observe relatively large pores, about 200 nm in dimensions, and small pores in the isthmuses between large pores. The results of studies of the luminescence spectra of

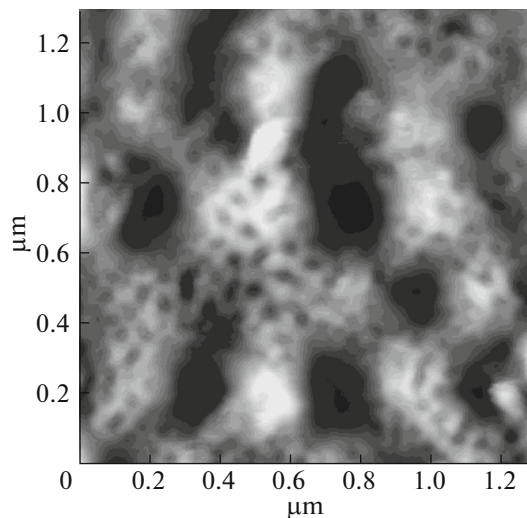


Fig. 5. AFM image of a single-layer tin-dioxide matrix.

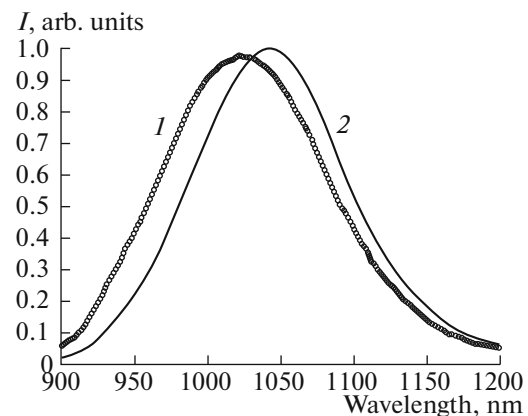


Fig. 6. PL spectra of CQDs deposited from solution 950 onto tin-dioxide substrates (1) with and (2) without annealing.

PbS QDs deposited onto such structures show a shift of the wavelength corresponding to the peak, as in the case of por-Si (Fig. 6).

Thus, in the studies, it is found that interactions between quantum-confined elements of the por-Si–PbS QDs system bring about a shift of the PL spectrum of por-Si to longer wavelengths.

Another result of the interactions is a change in the PL properties of PbS QDs. It is established that the lead-sulfide QDs produced by chemical deposition onto matrices fabricated from porous silicon and metal–oxide sol–gel structures exhibit efficient luminescence in the infra-red (IR) spectral region; however, the emission peak is shifted to shorter wavelengths. The structure and composition of the matrix induce a decisive effect on the luminescence spectra of the QDs, defining the emission wavelength.

ACKNOWLEDGMENTS

The work was supported by the Ministry of Education of the Russian Federation in the framework of the project of the state task in the field of scientific activity, project number 16.1307.2014K.

REFERENCES

1. L. Bakueva, S. Musikhin, M. A. Hines, et al., *Appl. Phys. Lett.* **82**, 2895 (2003).
2. O. A. Aleksandrova, A. I. Maksimov, E. V. Maraeva, et al., *Nano- Mikrosist. Tekh.*, No. 2, 19 (2013).
3. S. A. Tarasov, O. A. Aleksandrova, A. I. Maksimov, et al., *Izv. Vyssh. Uchebn. Zaved., Elektron.*, No. 3, 28 (2013).
4. I. I. Mikhailov, S. A. Tarasov, A. V. Presnyakova, and D. S. Romanovskii, *Izv. SPbGETU LETI* **5**, 22 (2013).
5. A. S. Lenshin, V. M. Kashkarov, Yu. M. Spivak, and V. A. Moshnikov, *Mater. Chem. Phys.* **135**, 293 (2012).
6. A. S. Len'shin, V. M. Kashkarov, Yu. M. Spivak, and V. A. Moshnikov, *Glass Phys. Chem.* **38**, 315 (2012).
7. V. A. Moshnikov, I. E. Gracheva, V. V. Kuznezov, et al., *J. Non-Cryst. Solids.* **356**, 2020 (2010).
8. V. S. Levitskii, A. S. Len'shin, A. I. Maksimov, et al., *Sorbtsion. Khromatogr. Prots.* **12**, 725 (2012).
9. S. A. Tarasov, I. E. Gracheva, K. G. Gareev, et al., *Izv. Vyssh. Uchebn. Zaved., Elektron.*, No. 2, 21 (2012).
10. S. A. Tarasov, I. E. Gracheva, K. G. Gareev, et al., *Semiconductors* **46**, 1584 (2012).

Translated by E. Smorgonskaya